The 2015 World Congress on
Advances in Structural Engineering and Mechanics (ASEM15)
Incheon, Korea, August 25-29, 2015

Reliability analysis of Integral Abutment Bridge under Seismic Load

Narges Easazadeh Far[1)] and Majid Barghian[2)]

[1)] *Department of Structural Engineering, Seraj Higher Education institute, Tabriz, Iran*
[2)] *Department of Structural Engineering, Faculty of Civil Engineering, Tabriz University, Tabriz, Iran*
[1)] easazadehfar@tabrizu.ac.ir
[2)] barghian@tabrizu.ac.ir

ABSTRACT

An Integral Abutment Bridge (IABs) is a jointless bridge that by eliminating expansion joints in deck and bearings, most of problems associated whit these joints have been removed. Among the loads act on these bridges, duo to the integrity of these structures, the seismic load is important and has deterministic role of this bridge performance. As, all developed bridge design codes have essentially been set for conventional bridges with expansion joints, evaluating the safety level of IABs designed by these codes is important. In this paper, the safety of IABs - designed by AASHTO LRFD bridge designed code - under seismic load is determined. For this purpose, by using reliability analysis of an IAB designed by AASHTO LRFD under seismic load, the reliability indexes for the bridge's 75 years design life have been calculated. The reliability indexes were calculated for bending and shearing limit states of the pile foundation by using Monte Carlo Method. For five considered earthquake sites, the calculated average reliability index for pile bending and shearing were obtained equal to 2.28 and 2.33, respectively.

Keywords: Reliability analysis, Integral abutment bridge, Seismic Load

1. Introduction

Integral abutment bridges (IABs) are continuous single or multi spans bridges in which the jointless superstructure is connected rigidly to the abutment. The rigid connection between them leads most of displacements and loads transfer from superstructure to substructure consisted of abutments and piled foundations. By eliminating the expansion joints in IABs, most of problems associated with expansion joints and bearings are removed. These advantages of IABs have caused them to be used throughout the world increasingly, especially, in USA, Canada, UK and South Korea. These bridges similar to conventional bridges are subjected to primary loads

---

[1)] Ph. D
[2)] Ph. D

(live loads, dead loads, seismic loads, etc.) and secondary effects (shrinkage, creep, passive pressure, uniform temperature changes, thermal gradients, etc.). Among these loads - due to the integrity of these bridges and the resultant complexity of soil-structure interactions - uniform thermal and longitudinal seismic loads become important and have deterministic role in the behavior of IABs.

Several researchers studied the behavior of these bridges under thermal and seismic loads, and showed the importance of these loads on the IAB's response. Tsang NCM and England GL (2002) investigated the Soil/structure interaction of integral bridge with full height abutments. Dicleli M and Albhaisi SM. (2004), studied the effect of cyclic thermal loading on the behavior of steel H-piles foundation of integral bridges. In this research the abutments of bridges are stub. Kim W. and Laman JA. (2010), investigated the Integral abutment bridge response under the thermal loading. In the other research they studied the long-term behavior of integral abutment bridges by using numerical analysis. Tegos and *et al*. (2005) proposed two different abutment configurations to improve seismic behavior of integral bridges. Itani and Pecan (2011) studied the seismic behavior of steel integral bridges and developed seismic design guidelines. Frosch and *et. al.* (2008) investigated the seismic behavior of IABs and developed design recommendations. Maleki and Mahjubi (2010) introduced a 2D finite element model for seismic analysis of retaining walls and integral bridge abutments. They also, proposed a new seismic soil pressure distribution to replace the Mononobe-Okabe (1929) equations. Kim (2010) proposed new load combinations for the load and resistance factor design (LRFD) to design typical IABs, by developing the nominal IAB response prediction models and establishing of IAB's response statistics using Monte Carlo simulation.

As other developed bridge design codes; American Association of State Highway and Transportation Officials (AASHTO LRFD) (2012) consider earthquake load separately in the Extreme Event I load combination as addressed equation 1. Evaluating the safety level of IABs designed by these codes is important for the following reasons:

As the load combinations of these codes have been primarily defined for conventional bridges with expansion joints, while due to the elimination of expansion joints and due to the integration between substructure and superstructure of IABs overall performance of bridges is different from conventional bridges. On the other hand, seismic load has played a decisive role in the behavior of bridges. Therefore, evaluating the safety level of IABs - designed according to AASHTO LRFD code under seismic load - is important.

In this paper, by using structural reliability analysis conducted on a case study bridge - designed in accordance with existing AASHTO LRFD code – under seismic load, the safety level of bridge was evaluated during its 75-year design life (AASHTO LRFD 2012):

$$\text{Extreme Event I} = \gamma_{DL} DL + \gamma_{P_a} P_a + \gamma_{\Delta P_a} \Delta P_{ae} + \gamma_{EQ} EQ \tag{1}$$

Where, *EQ, DL,* P_a, ΔP_{ae} are seismic load, dead load, static earth pressure and seismic earth pressure, respectively and γ_{DL}=1.25, γ_{pa} = 1.5, $\gamma_{\Delta pa}$ = 1, γ_{EQ} = 1 are the considered load factors.

To evaluation the safety of IABs under seismic load, an basic IAB designed based on AASHTO LRFD Bridge design specification (2012) was analyzed to calculate the

reliability index value under seismic load for its 75 years design life (According to AASHTO LRFD (2012), a 75 years design life is used for an IAB). The analyses consider the structural safety as well as pile foundation safety. As pile bending moment and shearing force are affected the most by the seismic load, the bending and shearing limit states of pile foundation are considered to evaluation of the bridge safety.

The statistical data required for this reliability analysis are assembled from reliability literature, Ghosn, M *et al*. (2003), United States Geological survey (USGS) website (2013).

2. Basic Concepts of Structural reliability theory

The purpose of the structural reliability theory is, including the uncertainties associated with the member capacity and the occurrence, intensities and effect of loads that the members are subjected to them during their design life. Thus, all variables contributing in the member resistance and the load effects should be represented by random variables. The minimum characteristics to define a random variable, R, are probability distribution function, PDF, the Mean value, $\overline{R}$ and the standard deviation, σ_R. As shown in Eq. (2), the Coefficient of variation (*COV*) is defined as the ratio of standard deviation, σ_R to mean value, $\overline{R}$ and bias factor, b_r as the ratio of the mean value, $\overline{R}$ to the nominal or design value, R_n.

$$COV = \frac{\sigma_R}{\overline{R}} \quad , \quad b_r = \frac{\overline{R}}{R_n} \tag{2}$$

Based on structural reliability theory, the safety of a structure can be achieved just when the structural resistance (R) exceeds the load effects (S). So, the reliability, R_e, of a structure is the probability of this exceedance, as follows:

$$\begin{aligned} &R_e = \Pr[R > S] \\ &R_e = \Pr[Z = R - S > 0] \\ &\text{or } R_e = \Pr[Z(X_1, X_2, ..., X_n) > 0] \end{aligned} \tag{3}$$

where Z is the limit state function that relates the resistance (R) to the load effects (S) for evaluating the safety level of the structure. X_1, X_2,..., X_n are the random variables associated with the resistance and the applied loads. In contrast, probability of failure, P_f, is the probability that the safety margin, Z, is less than zero, as follows:

$$P_f = \Pr[R < S] = \Pr[Z < 0] = 1 - R_e \tag{4}$$

The reliability index, β, is usually used to evaluate the safety level of a structure. This index is related to the probability of failure as follows:

$$\beta = -\Phi^{-1}(P_f) \tag{5}$$

where Φ is the cumulative standard normal distribution function. A general equation for the probability of failure is defined as follows:

$$P_f = \int_{Z(\{\boldsymbol{X}\})<0} f_{\{\boldsymbol{X}\}}(\{\boldsymbol{x}\}) dx_1 dx_2 ... dx_n \tag{6}$$

where $\{\boldsymbol{X}\} = \{ X_1, X_2,...,X_n\}$ is a random variables vector, $f_{\{\boldsymbol{X}\}}(\{\boldsymbol{X}\})$ is the probability density of vector $\{\boldsymbol{X}\}$ and $Z(\{\boldsymbol{X}\})$ is the limit state function. As $f_{\boldsymbol{X}i}$ is generally unknown, the evaluation of the probability of failure, P_f, using Eq. (6) is very difficult. Therefore, based on the type of distribution function corresponding to the structural resistance (R) and load effects (S) in the limit state function (Z) in Eq. (3), there are several methods to evaluate the reliability index. The methods include: the first order reliability method (FORM), the second order reliability method (SORM) and Monte Carlo simulation Method, etc. In this paper, the Monte Carlo simulation method was used to evaluate the probability of failure. Then by using Eq. (5), the reliability index was obtained. The Monte Carlo method creates large number simulated outcomes of a limit state. Next, by counting the number of failure events ($Z < 0$) and dividing them into the total number of simulated events, the probability of failure, $P_{f,}$ can be estimated. In this method, during each simulation, all involved variables in the limit state function are chosen (or generated) randomly (Lemaire, Maurice. 2009).

The reliability index has been used to express structural risk. For this index the range of 2 to 4 is usually specified to failure of a single component for different structural application (Ghosn, M e*t al*. 2003).

To calculate the reliability index, at first, the statistical data for all the random variables associated with the limit state function Z of Eq. (3) should be obtained. These data including all the uncertainties in estimating the member resistances and the load effects. According to Nowak (1999) and Ellingwood et al. (1980) approach a bridge member resistance capacity by a variable R can be defined as follows:

$$R = M\ F\ P\ R_n \tag{7}$$

where M is material factor representing properties such as strength, modulus of elasticity, etc; F is fabrication factor including geometry, dimensions, and section modulus; P is analysis factor such as approximate models for estimating member capacity, idealized stress and strain distribution models; and R_n is predicted member capacity using code-specified methods. Eq. (7) can be used to find the mean value of R using Eq. (2) if the total resistance bias, b_r, is set to be equal to the product of the mean values of M, F, and P. The resistance model of Eq. (7) does not directly account for member deterioration or other changes with time. Thus, all the variables are time-independent random variables.

For a bridge member (or structural system) to be safe, the resistance should be large enough to the maximum load effect that could occur within the structure's service life. Estimating the effects of the maximum loads involves a number of random variables, which may often be associated with large levels of modeling uncertainties. In particular, the intensities of the maximum loads are time-dependent random variables in the sense that longer service lives imply higher chances that the structure will be subjected to a given extreme load level. On the other hand, the projection of limited load intensity data, collected from previous measurements over short periods of time, to future return periods is associated with various levels of statistical modeling uncertainties. In addition, modeling the structure's response to the applied loads and estimating the variables that

control the effects of the loads on the structure are associated with high levels of uncertainty that are independent of the return period. These modeling uncertainties are often represented by time-independent random variables. Thus, the effect of a particular load type, *i*, on a structural member may be represented as follows:

$$S_i = \lambda_i f_i(\lambda_{Qi} C_{ij} Q_i) \tag{8}$$

where S_i is the load effect for load type *i*; λ_i *is* the analysis modeling factor that accounts for differences between measured load effects and predicted load effects; f_i ( ) is the analysis prediction model that converts load intensities into load effects; Q_i is the projected intensity variable of load type *i* for the return period of interest; λ_{Qi} is the statistical modeling variable that accounts for the limitations in predicting the value of Q_i; and C_{ji} is the analysis variables such as bridge material and geometrical properties required for executing the analysis for load type *i*. All the variables in Eq. (8) may be considered random where Q_i is a time-dependent random variable and the remaining variables are time-invariant. The probability density of the load intensity, Q_i, for a given return period, *t*, can be calculated by studying the probability that Q_i will exceed a given value within *t*. Assuming that the occurrence of load events follows a Poisson model, the probability that the load intensity will exceed a value x, within a period, *t*, is represented by: (1-$F_{Qi,t}$[*x*]), which may be approximated as

$$\Pr(Q_i > x; T < t) = 1 - F_{Q_{i,t}}(x) = 1 - e^{(-tp)} \tag{9}$$

where *p* is the rate of exceedance per unite time. *P* is equal to the probability of exceeding *x* when *t* equals 1.0:

$$p = \Pr(Q_i > x) = 1 - F_{Q_i}(x) \tag{10}$$

For extreme values of *x* ,when the value of F_{Qi}(*x*) are close to 1.0, and *p* is calculated for one unit of time while the return period, *t*, consists of *m* units of time, Eq. (9) can be approximated as

$$\begin{aligned} \Pr(Q_i > x; T < t) &= 1 - F_{Q_{i,t}}(x) = 1 - e^{(-tp)} \approx 1 - (1-p)^m \\ &= 1 - (F_{Q_i}(x))^m \end{aligned} \tag{11}$$

Eq. (10) can be written as follows:

$$\Pr(Q_i < x; T < t) = F_{Q_{i,t}}(x) \approx (F_{Q_i}(x))^m \tag{12}$$

Eq. (12) indicates that the cumulative probability function for a return period of time, *t*, may be approximated by raising the cumulative probability function of the basic time period to the power, *m*.

3. IAB Pile Resistance Capacity

As described before, the considered limit state in this study is the bending moment and shearing failure of the IAB pile. For supporting the abutments of the considered IAB

a single row of steel H-piles are used. As the bending moment and shearing capacities of steel pile are defined by the its yield stress, F_y, and geometric parameters, by considering the yield stress of pile section as a random variable the uncertainties associated with the bending moment and shearing capacities of the pile are taken account during reliability analysis. So, for the yield stress, F_y, a bias of 1.05 and a COV of 10% using a Lognormal distribution are used (Galambos *et al.* 1978).

4. Reliability Models for Loads

According to Extreme Event I load combination of AASHTO LRFD (2012), nominal design loads dead load, earth pressure, seismic load are just considered in this study. The required statistical models of these loads are described in this section.

4.1 Dead Load

Based on Nowak (1999), the statistics for dead load are summarized in Table 1.

Table 1 Dead load Statistics (Nowak 1999)

Load	Bias factor (b_r)	Coefficient of variation (*COV* %)
Dead Load (factory-made component)	1.03	8
Dead Load (factory-made component)	1.05	10
Asphalt Wearing Surface (88.9 mm assumed)	1	25

Since in this study, the deck of considered IAB is a factory-made steel girder composite, and cast-in place concrete slab, therefore, a bias of 1.08 = 1.03 $\times$ 1.05 with a *COV* of 12.8 % = $\sqrt{10^2+8^2}$, using a normal distribution are used for dead load.

4.2 Backfill Earth Pressure

Backfill static earth pressure dependent on the movement direction of an IAB's abutments under applied loads can be the form of passive or active. The backfill passive pressure (Abutment moves far from backfill) resists bridge against applied load while active pressure (Abutment moves toward backfill) is a permanent load on the abutments. Based on Rankin's theory, the lateral earth pressure considering cohesion-less backfill soil is determined by unit weight and fraction angle of soil. Based on Becker's researches (1996), statistics for backfill soil are summarized in Table 2.

Table 2 Backfill Soil related statistics (Becker 1996)

Variable	Bias	COV	Distribution type
Unit Weight (γ)	1.0	7 %	Normal
Fraction Angle (ϕ_S)	1.0	13 %	Normal
Rankine Coefficient (K_P, K_a)	1.5	20 %	Normal
Cyclic effects, λ_{cyc}	1.0	15 %	Normal

4.3 Earthquake load

The reliability analysis of a structural member under earthquake load involves a number of random variables that the uncertainty of them should be considered. A brief discussion of each variable is given and statistics for each are summarized in Table 3.

4.3.1 Intensity of Earthquake Acceleration

The expected earthquake intensity for IAB's sites was obtained from the USGS maps (2013). These maps provide the horizontal peak ground accelerations (PGAs) for various sites throughout the United States with 7 percent exceedance probability in 75 years (a return period of about 1000yr). In this study five sites were considered as the IAB's site: San Francisco with 94117 zip code, Seattle with 98195 zip code, Memphis with 38101 zip code, New York whit 10031 zip code and St. Paul whit 55418. An annual exceedance probability curves for PGA was provided by Frankel *et al*. (1997) for a number of sites (see Fig. 1).

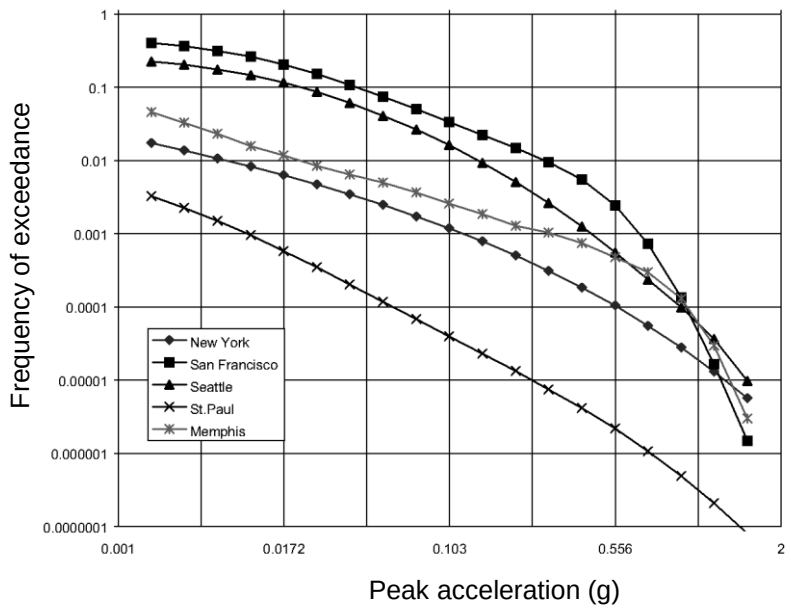

Fig. 1 Annual probability of exceedance curves for PGA (Frankel *et al*. 1997)

4.3.2 Rate of earthquake occurrence

The number of expected earthquakes varies from site to site and is available at the USGS website (2013). The average number of earthquakes in one year is about 8 for San Francisco, 2 for Seattle, 0.5 for Memphis (one every 2 years), 0.4 for New York (one every 2.5 years), and 9×10^{-3} for St. Paul (one every 111 years) .

4.3.3 Natural period of IABs

The natural period of an IAB is related to the type of bridge structure, type of bridge foundation, the characteristics of the used materials, the characteristics of bridge geometry, the interaction between soil and structure (SSI), etc. As the considered IAB in this study included the effects of SSI, based on published researches (Chopra *et al* 2000), a bias of 0.9 and a *COV* of 20% using a normal distribution was used for the natural period of the IAB.

4.3.4 Mass Applied

To account for uncertainties associated with the mass applied on the IAB's members (considering weight alone) a bias of 1.05 and a COV of 5% using a normal distribution were used (Ellingwood *et al.* 1980 and Nowak1999).

4.3.5 Seismic Response Coefficient

The design response spectrum proposed by AASHTO LRFD (2012) was used in this paper. These design spectra are based on the USGS mapping project (2013). For considering uncertainties associated with these spectra, the statistics provided by Frankel *et al.* (1997) was used. They found that for all sites inside USA, the mean value of spectral accelerations are very close to the design spectral accelerations; so a bias of 1.0 can be used. Also, for all sites, *COV* depends on the number of observed earthquakes at which, the *COV* is low for sites with high frequency of earthquakes and for sites with low frequency the *COV* is high. Therefore, for San Francisco, the *COV* is about 15%, for Seattle and Memphis is about 25%, for New York is about 30% and for St. Paul is about 40%. For this variable a normal distribution is used.

4.3.6 Modeling factor

Modeling factor was used to take into account for the uncertainties produced during the dynamic analysis process. A bias of 1 and a *COV* of 20% using a normal distribution were used for this variable (Ellingwood *et al.* 1980).

4.3.7 Reliability Equation for Earthquake Load

Using the presented information, the equivalent seismic load applied on the IAB is defined as follows:

$$F_{EQ} = \lambda_{eq} C' S_a(t'T) \times \frac{A \times W}{R_m} \tag{13}$$

where, F_{Eq} is the equivalent applied load, λ_{eq} is the modeling factor, C' is the response spectrum modeling parameter, A is the maximum 75-year peak ground acceleration at the site, S_a is the calculated spectral acceleration using the IAB's period, T, and period modeling factor, t', W is the weight of system and R_m is the response modification factor which is equal to 1.0 for IAB's pile (AASHTO LRFD (2012). The statistics for random variables used in Eq. (13) are summarized in Table 3.

5. Reliability Analysis of the Integral Abutment Bridge

In this section, the reliability analysis performs for a basic IAB designed to satisfy the current AASHTO LRFD specifications for evaluating the safety level under seismic load. For this purpose by using the Monte Carlo Method the reliability index, β, is calculated for considered bridge subjected to earthquake load. Geometric and structural properties of the basic IAB are described below.

Table 3 Earthquake load related statistics

Variable		Bias	COV	Distribution type	Reference
Earthquake Modeling factor, λ_{eq}		1.0	20%	Normal	(Ellingwood *et al*.1980)
spectrum modeling factor, C'	San Francisco	1.0	15%	Normal	(Frankel *et al*. 1997)
	Seattle		25%		
	Memphis		25%		
	New York		30%		
	St. Paul		40%		
75-year PGA, A	San Francisco	from Fig. 1	from Fig. 1	from Fig. 1	(USGS 2013)
	Seattle				
	Memphis				
	New York				
	St. Paul				
Period modeling factor, t'		0.9	20%	Normal	(Chopra *et al* 2000)
Weight, W		1.05	5%	Normal	(Ellingwood *et al*.1980)

5.1 Geometric an Structural Properties of the Basic IAB

The considered IAB in this study is a one-span 40 m IAB having the longitudinal section as shown in Fig. 2. The superstructure of the bridge is composed of concrete slab whit 20 cm thickness and steel beams at 2 m spacing. Each abutment of this bridge has 7 m height and 1 m wall thickness and supported on a single row of steel H piles with 12 m length at 1 m spacing. The section properties of deck girder and piles are given in Table 5.

The abutments backfill soil is assumed to be dense cohesion-less soil with 30° angle of internal friction and a unit weight of 16.72 kN/m^3.

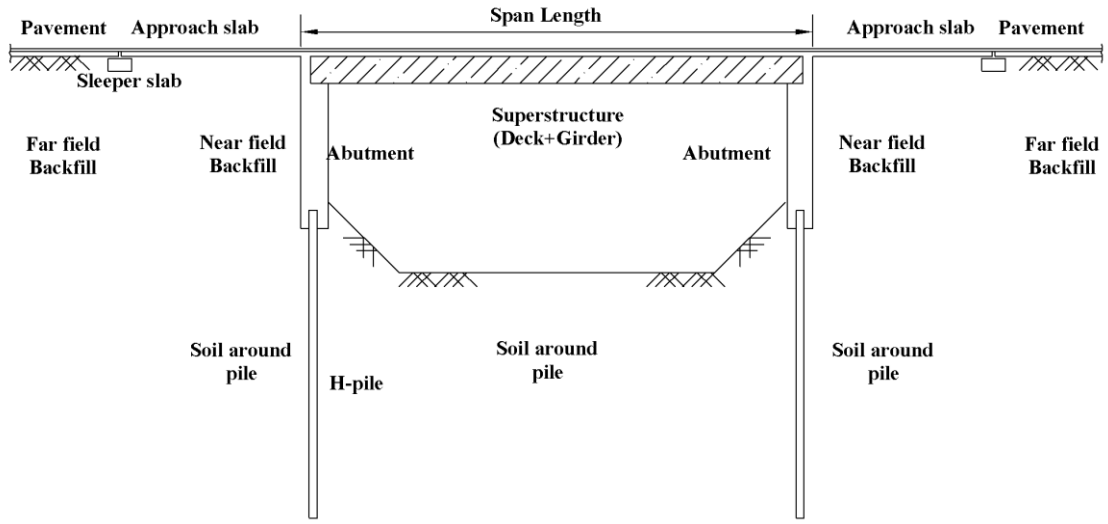

Fig. 2 Longitudinal section of the IAB

Table 5 Steel sections properties

Section		Size	Height (cm)	Flange width (cm)	Flange thickness (cm)	Web thickness (cm)
Girder		W 1000×975	111	43	9	5
Piles	San Francisco	H 300×300×15×15	30	30	1.5	1.5
	Seattle	H 300×300×12×12	30	30	1.2	1.2
	Memphis	H250×250×9×14	25	25	1.4	0.9
	New York	H200×200×12×12	20	20	1.2	1.2
	St. Paul	H200×200×8×12	20	20	1.2	0.8

As described earlier, the piles moment and shear force are affected the most by the earthquake load, thus, in this study bending moment and shearing failure limit state of the IAB piles at point *A* (where the pile connect to abutment) were considered for reliability analysis. The requirement moment and shear capacity was calculated to satisfy the current AASHTO LRFD specifications. The free body diagram of the basic IAB pile under applied load is shown Fig. 2. where, F_{DL} = 198.16 kN is the permanent weight of superstructure, M_{DL} = 1.32 MN is the moment caused by the permanent weight of superstructure, P_a = 272.82 kN is the static active backfill force and acts on the H/3 from the bottom of abutment, ΔP_{ae} is the seismic active backfill force based on Mononobe, *et al*. 1929 and Okabe 1926, and for San Francisco, Seattle, Memphis is equal to 819.33 kN, for New York is equal to 166.28 kN and for St. Paul is equal to 17.27 kN. This load acts on the 0.6 H from the bottom of abutment (Seed, H. *et al.* 1970), H = 7 m is the abutment height, e_1 = 0.25 m is the deal load eccentricity from the point *A*, F_{EQ} is the equivalent earthquake force - described below - transferred from the IAB deck and acts on the distance, f = 0.25 m from the bottom of abutment.

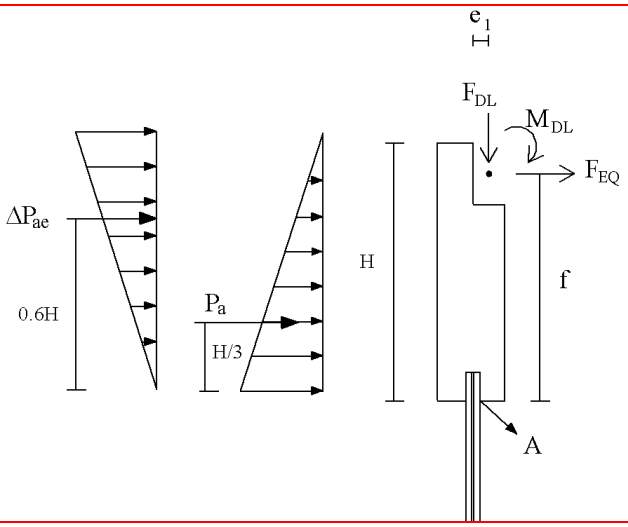

Fig. 3 Free body diagram of IAB pile, dominant failure is bending at point *A*

The equivalent internal earthquake force, F_{EQ} , by Using the nominal natural period of the T = 0.41s, the soil of type *D* and the calculated spectra acceleration for 1000-year return period (7% probability of exceedance in 75 years) is obtained as follows:

$$F_{EQ} = \frac{S_a \times W}{R_m} \tag{14}$$

where S_a is the spectral acceleration, W is the weight of structure and R_m is the response modification factor. Based on AASHTO LRFD (2012) by Using a modification factor R_m = 1 the equivalent earthquake is equal to 307.54 kN for San Francisco site, 210.52 kN for Seattle, 176.38 kN for Memphis, 44.05 kN for New York and 10.51 kN for St. Paul.

As the dominant AASHTO LRFD (2012) load combination to design the considered pile is the Extreme Event I combination at point *A* (see Fig. 3), the design equation used for calculating the nominal moment capacity is as follows:

$$\phi M_{req} = 1.25M_{DL} + 1.5M_{P_a} + M_{\Delta P_{ae}} + M_{EQ} \tag{15}$$

where ϕ is the resistance factor which for bending is equal to 0.9, M_{DL} = 1.37 MN-m (= 0.198 × 0.25 + 1.32) is the total moment caused by permanent weight of superstructure, M_{Pa} = 0.64 MN-m (= 0.273 MN × 2.333 m) is the moment caused by static active backfill force, $M_{\Delta Pae}$ is the moment caused by seismic active backfill force and is equal to 3.44 MN-m (= 0.819 MN × 0.6 × 7 m) for San Francisco, Seattle, Memphis, equal to 0.698 MN-m for New York and equal to 0.0725 MN-m for St. Paul. M_{EQ} is the equivalent earthquake moment that equal to 1.85 MN-m for San Francisco, 1.26 MN-m for Seattle, 1.058 MN-m for Memphis, 0.264 MN-m for New York and 0.063 MN-m for St. Paul.

Based on the Extreme Event I combination at point *A* (see Fig. 3), the design equation used for calculating the nominal sheer capacity is as follows:

$$\phi V_{req} = 1.25V_{DL} + 1.5V_{P_a} + V_{\Delta P_{ae}} + V_{EQ} \tag{16}$$

where, ϕ is the resistance factor which for shearing is equal to 0.9, V_{DL} is the total shear caused by permanent weight of superstructure and usual 0, V_{Pa} = 0.272 MN is the shear caused by static active backfill force, $V_{\Delta Pae}$ is the shear caused by seismic active backfill force and is equal to 0.819 MN for San Francisco, Seattle, Memphis, equal to 0.166 MN for New York and equal to 0.0172 MN for St. Paul. V_{EQ} is the equivalent earthquake Shear that equal to 0.308 MN for San Francisco, 0.211 MN for Seattle, 0.176 MN for Memphis, 0.044 MN for New York and 0.0105 MN for St. Paul.

Using Eq. (15) the requirement moment capacity, M_{req} is equal to 8.84 MN-m for San Francisco, 8.18 MN-m for Seattle, 7.96 MN-m for Memphis, 4.024 MN-m for New York and 3.12 MN-m for St. Paul. Using Eq. (16) the requirement sheer capacity, V_{req} is equal to 1.706 MN for San Francisco, 1.6 MN for Seattle, 1.56 MN-m for Memphis, 0.69 MN for New York and 0.49 MN for St. Paul.

5.2 Reliability Analysis Under seismic load

The reliability analysis of the IAB pile is performed using the models described in section 4 and the free body diagram shown in Fig. 3. Referring to Fig. 3 the failure function for pile bending can be represented by following equation:

$$Z_M = M_{Pile} - (M_{DL} + \frac{\gamma \times H^2 \times K_{ae} \times b}{2} \times \frac{H}{2} \times \lambda_{cyc} + F_{EQ} \times f) \tag{17}$$

where M_{Pile} is the pile bending moment capacity, M_{DL} is the total Moment caused by superstructure weight, F_{EQ} is the equivalent earthquake load transferred from superstructure defined by Eq. (13), γ is the specific weight of backfill soil, K_{ae} is the seismic active earth pressure coefficient (Mononobe, *et al*. 1929 and Okabe 1926), H = 7 m is the abutment height, b = 2 m is the abutment wide corresponded to each considered pile, f = 6 m is the distance earthquake load from point *A* and λ_{cyc} is the model of the effect of cyclic loading on the pile.

Based on Figure 4, the failure equation for pile sheering can be represented as follows:

$$Z_V = V_{Pile} - (\frac{\gamma \times H^2 \times K_{ae} \times b}{2} \lambda_{cyc} + F_{EQ}) \tag{18}$$

where V_{Pile} is the pile sheering capacity.

Referring to Eqs. (16)-(17), failure occurs when Z_M or Z_V are less than zero. All variables in Eqs. (16)-(17) are considered random expect for abutment height, H, abutment wide corresponded to each pile, b and distance earthquake load from point *A*, f. The statistical models used to describe the random variables are provided in tables 1, 2 and 3. In these failures limit state only earthquake load composed of time-depended and time-in depended random variables. The reliability analysis of the IAB pile was performed for five sites by using Monte Carlo simulation method. Figs. 4-5 show the reliability index for the bending and shearing failure limit states for each of five sites as a function of pile moment and sheer capacity, respectively. The abscissa of the plot is

normalized such that a ratio of 1.0 indicates that the bridge is designed to exactly satisfy the AASHT LRFD (2012) specifications requirements. Fig. 4 shows that the AASHTO LRFD (2012) specifications using a nominal response modification factor R_m = 1 for pile bending limit state will produce a reliability index, β, between 2.12 and 2.57. The average from the five sites is equal to 2.28. Fig. 5 shows that for pile shearing limit state the average reliability index for five sites is 2.33 with a minimum index equal to 2.09 and a maximum value equal 2.68.

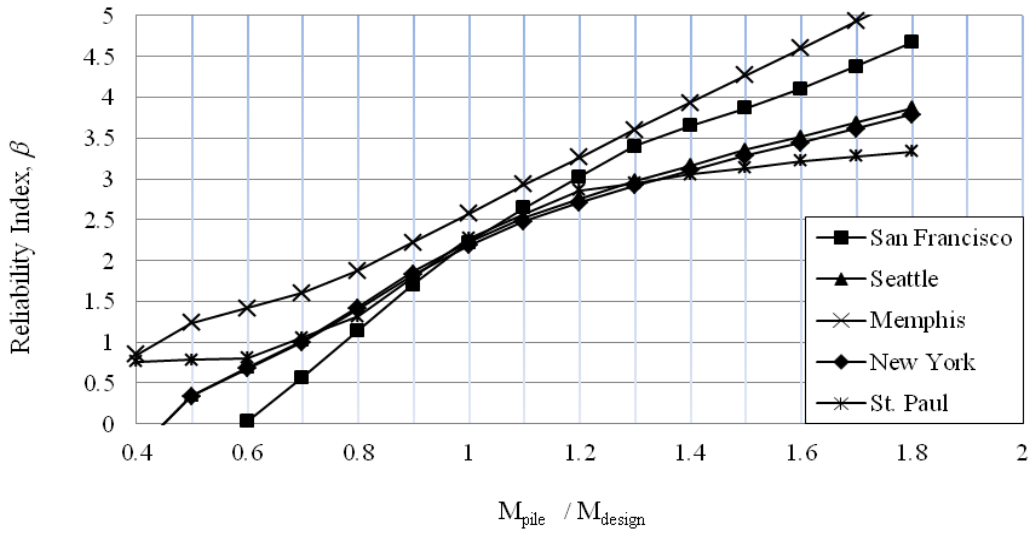

Fig. 4 Reliability index for bending of considered IAB's pile under earthquake loads

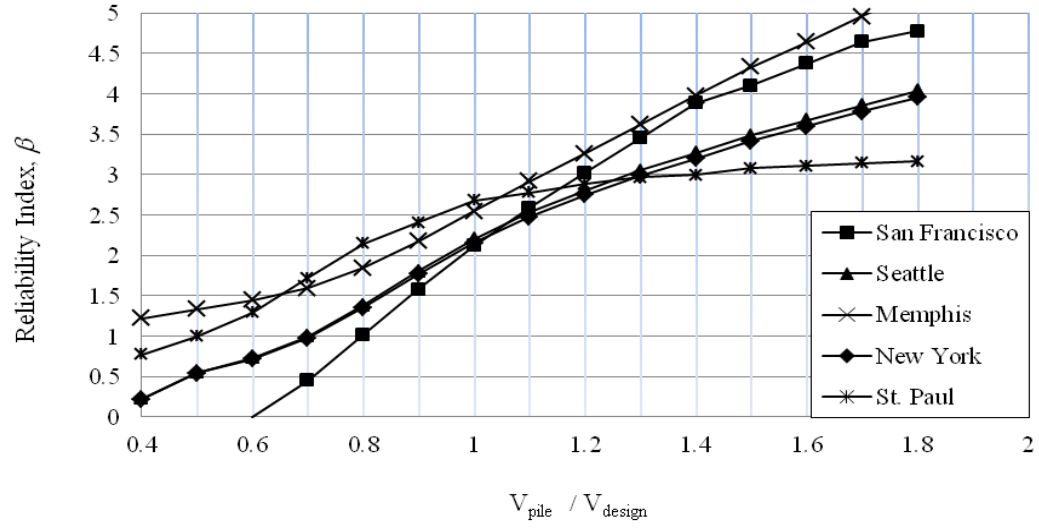

Fig. 5 Reliability index for shearing of considered IAB's pile under earthquake loads

9. Conclusion

Integral abutment bridges (IABs) are jointless bridges that by eliminating the expansion joints have many advantages over conventional bridges. Duo to the integrity of these bridges, among the loads act on these bridges, seismic loads have major role to design of these bridges and readily transferred to substructure and affect the design of these components. As, all developed bridge design codes have been primarily defined for conventional bridges with expansion joints and the behavior of the IABs is differ complete from conventional bridges, the evaluating the safety level of IABs designed by these codes is important. In this paper, by concerning the safety of the pile foundation of an IAB designed by AASHTO LRFD bridge designed code under seismic load, the safety level of IABs under Seismic loads has been evaluated. By using Monte Carlo Reliability analysis method, the reliability indexes for the bridge's 75 years design life have been calculated. The Reliability indexes were calculated for bending and shearing limit states of the pile foundation. For five considered earthquake sites, the calculated average reliability index for pile bending and shearing were found to be equal 2.28 and 2.33, respectively. These indexes are in the range of 2 to 4 that is usually specified to failure of a single component for different structural application to express structural risk by many code-writers.

References

Tsang NCM, England GL. (2002), “Soil/structure interaction of integral bridge with full height abutments”, *Proceedings of the 15th ASCE Engineering Mechanics Conference*, Columbia University, NY.

Dicleli M, Albhaisi SM. (2004), “Effect of cyclic thermal loading on the performance of steel H-piles in integral bridges with stub-abutments”, *J Constructional Steel Research*, **60**(2): 161-182.

Kim W and Laman JA. (2010), “Integral abutment bridge response under thermal loading”, *Engineering Structures*, **32**: 1495-1508.

Tegos I, Sextos A, Mitoulis S, Tsitotas M. (2005), “Contribution to the improvement of seismic performance of integral Bridges”, *Proc 4th European Workshop on the Seismic Behavior of Irregular and Complex Structures*; Thessaloniki, Greece.

Itani A, Pekcan G. (2011), “Seismic performance of steel plate girder bridges with integral abutments”, *Publication No. FHWA-HIF-11-043*.

Frosch, RJ, Kreger ME, Talbott AM. (2009), “Earthquake resistance of integral abutment bridges”, *Publication FHWA/IN/JTRP-2008/11*. Joint Transportation Research Program, Indiana Department of Transportation and Purdue University, West Lafayette, Indiana. Doi: 10.5703/1288284313448

Maleki S, Mahjoubi S. (2010), “A new approach for estimating the seismic soil pressure on retaining walls”, *J Scientia Iranica*., **17**(4): 273-284.

Mononobe, N., and Matsue, H. (1929), “On the determination of earth pressures during earthquakes”, *Proc., World Engrg.* Conf., 9, 176.

Kim W. (2008), “Load and resistance factor for integral abutment bridges”, Ph.D. dissertation, PA: Pennsylvania State University, University Park.

Design code (2012), *AASHTO LRFD Bridge Design Specifications*, American Association of State Highway and Transportation Officials. Washington (DC).

Ghosn, M., Moses, F., and Wang, J. (2003), "Design of highway Bridges for Extreme Events", *NCHRP Report 489*, Transportation Research Board of the National Academics, Washington, DC.

U.S. Geological Survey Website, (2013) *USGS*, http://earthquake.usgs.gov/earthquakes.

Lemaire, Maurice. (2009), *Structural Reliability*, Published by ISTE Ltd and John Wiely & Sons, Inc., London SW19 4EU, UK and Hobokon, NJ 07030, USA.

Nowak, A.S. (1999), "Calibration of LRFD bridge design code", *NCHRP Report 368*, Transportation Research Board of the National Academies, Washington, DC.

Ellingwood B, Galambos, T.V., MacGregor, J.G., and Comell, C.A. (1980), "Development of a probability based load criterion for American national standard A58", *National bureau of standards*, Washington, DC.

Galambos, T. V. and Ravindra, M. K. (1978), "Properties of steel for use in LRFD", *Journal of the Structural Division, ASCE*, **104**(9), 1459-1468.

Becker, D.E. (1996), *18th Canadian Geotechnical Colloquium*: "Limit States Design for Foundations". *Part II Development for the National Building Code of Canada, Canadian Geotechnical Journal*, Vol. 33; pp. 984–1007.

Frankel, A., Harmsen, S., Mueller, C., Barnhard, T., Leyendeker, E.V., Perkins, D., Hanson, S., Dickrnan, N., and Hopper, M. (1997), *USGS National Seismic Hazard Maps*: "Uniform Hazard Spectra, De-aggregation, and Uncertainty", *Proceedings of FHWA/ NCEER Workshop on the National Representation of Seismic Ground Motion for New and Existing Highway Facilities*, NCEER Technical Report 97-0010, SUNY Buffalo, NY; pp. 39–73.

Chopra, A.K., and Goel, R.K. (2000), "Building period formulas for estimating seismic displacements", *EERI Earthquake Spectra*, Vol. 16, No. 2.

Okabe, S. (1926), "General Theory of Earth Pressure", J*. Japanese Soc. Of Civ. Engrs.*, Tokyo, **12**(1).

Seed, H. B., and Whitman, R. V. (1970), "Design of Earth Retaining Structures for Dynamic Loads", *Proc., the specialty Conference on Lateral Stresses in the Ground and design of Earth Retaining Structures*, ASCE; 47-103.